

Explicit calculations of homoclinic tangles in tokamaks

R. K. W. Roeder,^{a)} B. I. Rapoport,^{b)} and T. E. Evans
General Atomics, P.O. Box 85608, San Diego, California 92186-5608

(Received 25 June 2002; accepted 20 May 2003)

Explicit numerical calculations of homoclinic tangles are presented for a physically realistic model of a resonantly perturbed magnetic field in a tokamak. The structure of these tangles is consistent with that expected from the general theory of near-integrable Hamiltonian systems commonly studied with simple algebraic twist map models. In addition, understanding the structure of homoclinic tangles corresponding to the primary separatrix of a poloidally diverted tokamak allows one to make predictions of the locations and structure of magnetic footprints and heat buildup on the tokamak wall. These separatrix tangles undergo an interesting bifurcation sequence as the current through a set of error field correction coils is increased. Since this model of the magnetic field is very realistic, these features are expected to be experimentally verifiable. © 2003 American Institute of Physics. [DOI: 10.1063/1.1592515]

Although the wild patterns of intersecting invariant manifolds associated with hyperbolic fixed points of a Hamiltonian mapping have been studied for years,^{1–3} there is renewed interest in these structures for tokamak physics.^{4,5} The main reason for this renewed interest is that the geometry of homoclinic tangles in tokamaks can be used to make specific predictions about particle confinement and heat buildup on the tokamak wall. We present calculations of these homoclinic tangles in a sophisticated numerical model TRIP3D⁶ of a tokamak's magnetic field and show how some of these calculations result in physical predictions about the locations and patterns of heat build-up on the tokamak wall which may be verified by experiments in the near future.

The TRIP3D code was developed to model elongated flux surfaces in poloidally diverted plasmas, such as DIII-D,⁷ by extracting axisymmetric fields from EFIT EQDSK equilibrium files.⁸ In addition to providing an accurate representation of the flux surfaces due to external shaping coils EFIT solutions account for the magnetohydrodynamic (MHD) effects of plasma pressure and current profile distributions on the magnetic equilibrium (e.g., Shafranov shift) and are constrained by experimental magnetic and current profile data on DIII-D.

The magnetic field in TRIP3D is a composite of axisymmetric and nonaxisymmetric fields, those induced by the toroidal and poloidal coils, along with those induced by the plasma current and those induced by nonaxisymmetric sources such as the error correction or C-coils in DIII-D. A general discussion of error field correction coil usage in tokamaks is given in Ref. 9. The C-coil perturbation is based on the physical location of the coil with each loop of the coil modeled as 20 straight line filaments. The vector field from each filament at each point along the field line trajectory is calculated using a Biot–Savart algorithm. All the magnetic field sources are added to determine the total field within the

tokamak at each integration step. A detailed description of the TRIP3D and C-coil models is given in Ref. 6.

In this paper we will be interested in the Poincaré map of this model, TRIP3D_MAP, and its inverse which are obtained by integrating the field line through a given point in the Poincaré section one toroidal transit forward, or backward for the inverse.

To summarize: the TRIP3D_MAP is a model of the field in poloidally diverted tokamak that both uses realistic diverted plasma equilibria and an engineering quality perturbation coil model.

Having developed the TRIP3D_MAP, we verified that the expected homoclinic tangle structures surround some of the prominent magnetic islands. A phase portrait with a (4,1) resonant tangle and a detailed view of one of the x-points for this tangle are shown for the TRIP3D_MAP in Fig. 1, at a common level of C-coil perturbation (about that required to correct error fields in DIII-D). We have also calculated homoclinic tangles surrounding magnetic islands, similar to the one shown in Fig. 4, for an algebraic map, the Tokamap,¹⁰ which also models the magnetic field in a tokamak.

The homoclinic tangles resulting from a separatrix in the integrable (axisymmetric) system are of particular interest since they form the “barrier” between the field lines in the core of the plasma and the open field lines (outside of the separatrix in the scrape-off layer) which quickly hit the vacuum chamber wall.

There is an interesting sequence of bifurcations in the TRIP3D_MAP that happens in a plasma equilibrium state which has two primary x-points (i.e., a double null diverted equilibrium). With no perturbation from the C-coils, the system is integrable and one obtains the idealized separatrix topology which is free of homoclinic tangles. With a small level of C-coil perturbation current (300 amp-turns), the inner separatrix splits into a homoclinic tangle that does not interact with the invariant manifolds from the upper x-point as shown in Fig. 2. As the C-coil perturbation current increases past a certain number of amp-turns, $A(dr_{sep})$

^{a)}Permanent address: Department of Mathematics, Cornell University, Ithaca, New York.

^{b)}Permanent address: Harvard University, Cambridge, Massachusetts.

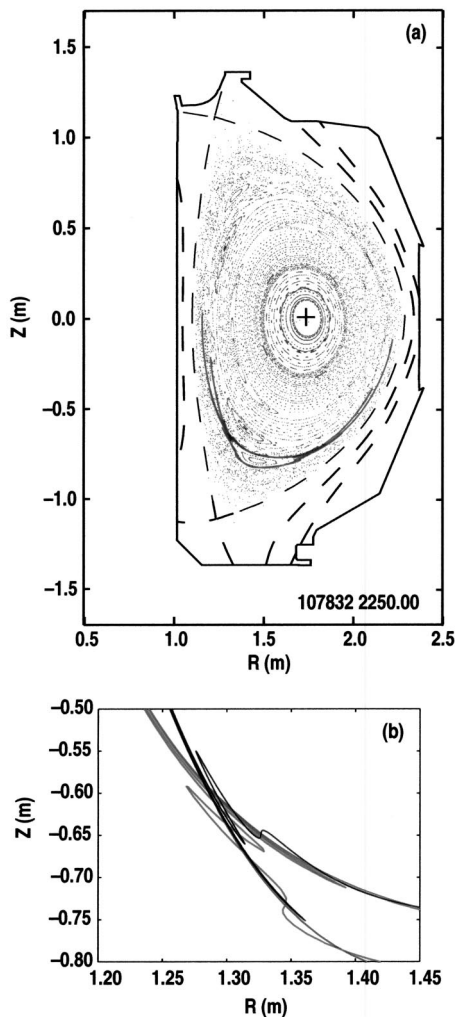


FIG. 1. (a) Phase portrait with a $(m,n)=(4,1)$ resonant tangle, and (b) a detail of one of the x-points of this tangle from the TRIP3D_MAP. The walls of the vacuum vessel are shown for reference.

which depends on the up-down symmetry of the equilibrium as parameterized by the dr_{sep} variable, the homoclinic tangle from the lower x-point crosses the invariant manifolds from the upper x-point, forming the behavior shown in Fig. 3. The reader should notice that it is not uncommon for C-coil currents to reach these levels for error field correction, and even reach 20000 amp-turns, so this bifurcation sequence is expected to take place in typical experiments.

The walls of the vacuum vessel are shown in Figs. 2 and 3, making the location and prominence of these tangles evident. These figures also indicate the importance of considering what happens where these tangles hit the walls of the vacuum vessel, as discussed below.

Understanding the specific details of particle transport across the separatrix of a modern poloidally diverted tokamak is fundamentally important to plasma confinement, since the plasma is “heated” inside of the separatrix, with losses due to particles that escape from this region and hit the vacuum chamber wall. It is certainly valuable to consider nondiffusive transport, since it occurs on a faster time scale than diffusive transport. The homoclinic tangle resulting

from an integrable separatrix is *the* mechanism for nondiffusive transport across the separatrix region.

People have studied transport across a separatrix region in many different ways^{11–13} but our calculations are the first that have been done for such a realistic approximation of the magnetic field. Figure 3 shows the trajectory of a field line that remains inside of the separatrix for a few toroidal transits before entering one of the interior lobes of the homoclinic tangle at the bottom of the tangle. With each subsequent iteration, the field line progresses from lobe to lobe (of the same orientation) counterclockwise around the tangle. Near the midpoint of the tangle, these lobes switch to being exterior lobes and force the field line outside of the separatrix. As the field line undergoes more toroidal transits, it progresses to the long and skinny lobes at the top of the tangle. As these lobes become infinitely long, the field line is forced into the upper wall of the vacuum vessel.

Particles following the field lines in the opposite toroidal direction will undergo similar motion, but entering the tangle in the interior lobes at the top of the tangle and hitting the lower plate of the vessel wall under sufficient toroidal transits. Some particles are also expected to escape through the tube-like region stretching from the lower x-point to the inner wall of the vacuum chamber.

The regions where magnetic field lines from deep within the tokamak hit the tokamak wall are known as “magnetic footprints”^{5,14,15} and are the regions where most of the particles transported across the separatrix are expected to hit. The lobes of the homoclinic tangle provide a constraint on the location of magnetic footprints, since field lines from the plasma core must remain within these lobes. Knowing the locations where the separatrix tangle hits the tokamak wall provides a good approximation of the gross structure of magnetic footprints. (Historically, magnetic footprints have been studied by following field lines directly instead of by calculated homoclinic tangles. However, concurrently with our work, other researchers have also considered this tangle-wall interaction.⁵)

It is expected that collisionless particles that escape from the hot plasma inside of the separatrix will follow field lines, and hence hit the wall of the vacuum vessel in the magnetic footprints, within the lobes of the separatrix tangle. Since the particles are typically hot, this lobe pattern may provide an explanation of the patterns of heat build-up on the walls of the vacuum vessel.^{16,17}

In a computational study similar to ours,¹⁵ the authors use a simple model for the three-dimensional vector field in a diverted tokamak to predict the two-dimensional structure of magnetic footprints. They detected “spiral-like” structures formed by stochastic field lines on the divertor targets. These spirals begin at some toroidal angle θ and some radius R and spiral inward accumulating at the circle of radius R_{sep} , where the separatrix would have hit the divertor plate. Although they did not use homoclinic tangles to calculate these magnetic footprints, these spirals are reminiscent of the lobe structure in homoclinic tangles. In fact, this is the same pattern as predicted by the locations where the homoclinic tangles that we have calculated hit the divertor plates. Thus,

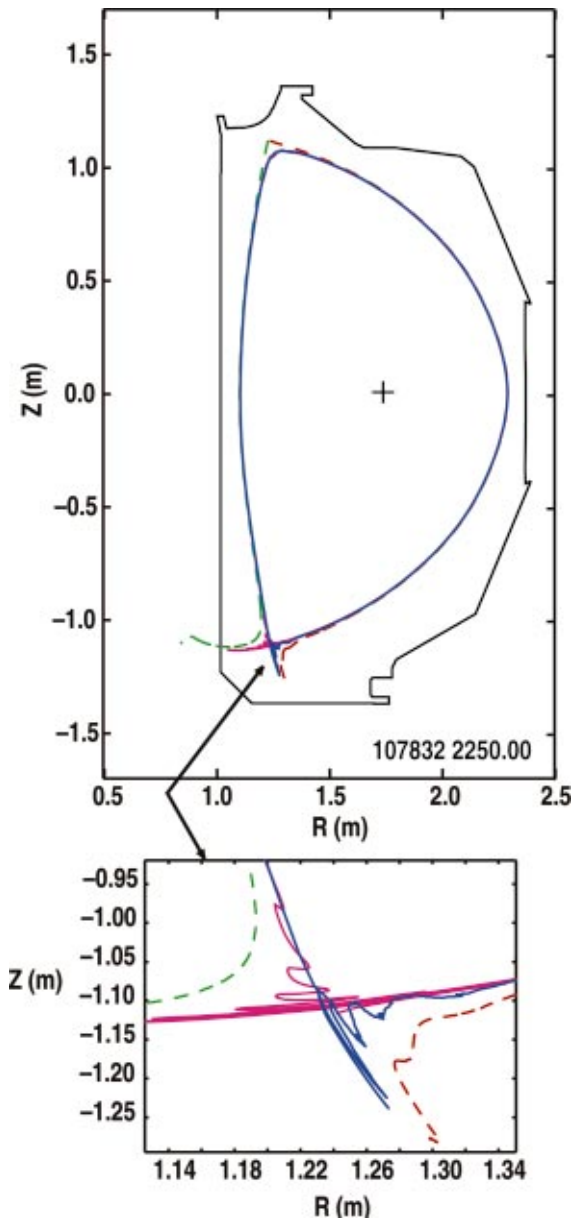


FIG. 2. (Color) Homoclinic tangle from the TRIP3D_MAP with a C-coil current of 300 amp-turns.

we suggest that the fuzzy “spiral-like” structure of magnetic footprints predicted in Ref. 15 are in fact a manifestation of the complex 3D topology prescribed by the homoclinic tangles predicted by our model. Here the boundaries of the footprints are formed by the invariant manifolds of the tangle’s lobes which determine the size and location of the footprints on various plasma-facing surfaces. At a C-coil current of 15000 amp-turns, we have computed this spiral structure on the divertor plates using the TRIP3D_MAP. Figure 4 shows the intersection of the homoclinic tangle lobes with the upper divertor plate, at $Z = 1.347$ m. Tangle intersections were calculated at a toroidal spacing of 10° , so that the spiral structure is clear. Notice that the spiral varies in width by a few cm, which is significantly bigger than the average ion Larmor radius at the plasma edge during a usual experiment in DIII-D.

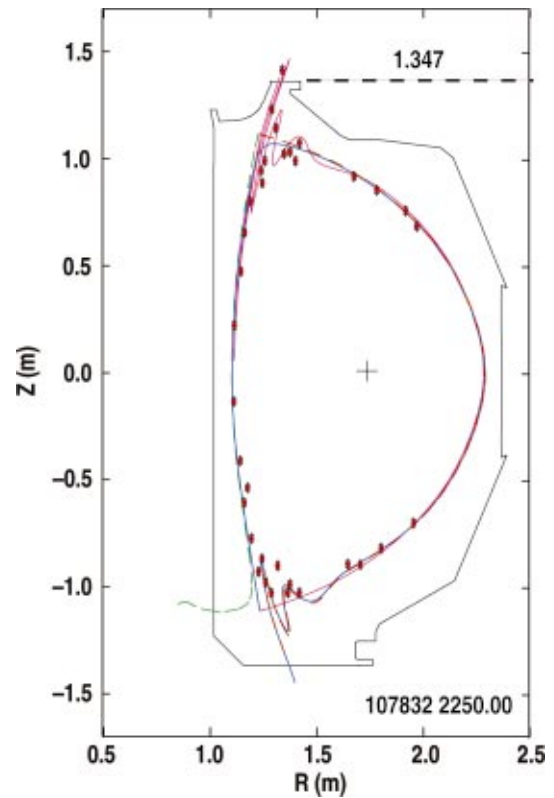


FIG. 3. (Color) Homoclinic tangle from the TRIP3D_MAP with a C-coil current of 10000 amp-turns. Large points plot a trajectory that escapes through the separatrix.

These primary separatrix tangles also define the flux loss channels for field lines that escape as a result of tangle overlap in resonant islands near the edge of the plasma in the high magnetic shear or so-called “pedestal” region. The loss of poloidal magnetic flux due to C-coil perturbations for various types of diverted equilibria in DIII-D is discussed in Ref. 6. It should be noted that the astonishingly complex topology displayed by homoclinic tangles was well under-

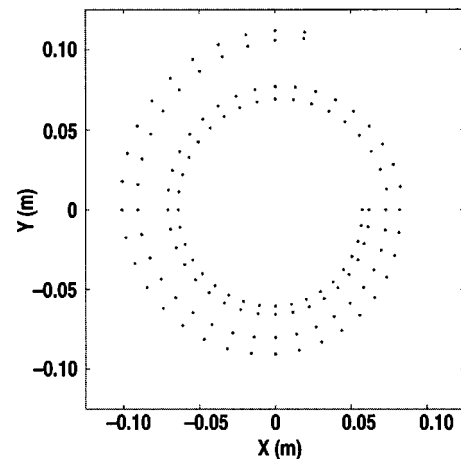


FIG. 4. The spiral formed by the intersection of homoclinic tangles, at a toroidal spacing of 10° , with the upper divertor plate, at $Z = 1.347$ m as shown in Fig. 3. The magnetic footprints must confine themselves within this spiral shape. Notice that we have subtracted 1.25 m from the radii, so that the spiral structure is more evident.

stood by Poincaré¹⁸ although he was unable to explicitly calculate and display them, even in the highly abbreviated form we have presented. Nevertheless, thanks to the availability of modern computers, computer graphics, and realistic mathematical models of the magnetic fields in tokamaks we now have the predictive tools needed to make detailed comparisons with experimental measurements such as those presented in Ref. 16.

Complicated predictions of the structure of magnetic footprints at specific toroidal angles have been calculated for circular plasmas using an elementary symplectic mapping to model the Poincaré map of a tokamak's magnetic field.⁵ As noted in Ref. 5, these patterns of heat flux can consist of a very complicated fractal structure since the lobe structure of a homoclinic tangles becomes complicated in the appropriate way as one computes the invariant manifolds to longer and longer lengths. While we are limited in the precision (and thus the length of tangles) that can be calculated in our model, we note that the first few lobes of the separatrix tangles do hit plasma-facing surfaces (at some toroidal locations) where one does not expect to observe high levels of heat flux. Thus, we expect that an experimental verification of the model can be made by using coils, such as the DIII-D C-coil, to rotate a tangle's toroidal phase and amplitude such that the footprint sweeps across the field of view of an infrared camera looking at a divertor target plate or plasma-facing component. We believe such an experimental verification of our model is reasonable based on the data shown in Ref. 16 and have proposed experiments of this type on DIII-D. As pointed out in Ref. 15 the impact of these features on the heating of plasma-facing surfaces increases with machine size so there is a certain amount urgency in developing a predictive understanding of these features for various operating regimes that are commonly accessible in DIII-D.

Also notice that the above analysis was of the situation in which the homoclinic tangle from the lower x-point intersects the invariant manifolds of the upper x-point [C-coil perturbation amplitude is greater than $A(dr_{sep})$]. In the case where the C-coil current is lower than $A(dr_{sep})$, the particles and heat are much less likely to escape and hit the upper walls of the vacuum vessel. The C-coils current can be controlled in each experiment, hence this bifurcation ought to be physically observable as the creation of a new magnetic footprint and the associated heat buildup on the upper tokamak wall when the C-coil current increases past $A(dr_{sep})$.

We have presented calculations of the homoclinic tangles structures in the TRIP3D_MAP model of a tokamak's magnetic field in an effort to confirm that the properties of this model agree with those expected from the general theory of homoclinic tangles in near-integrable systems. As expected from the generic properties of these structures, homoclinic tangles were found surrounding resonant islands as well as in the primary separatrices of unperturbed (integrable) double null diverted equilibria.

For poloidally diverted tokamaks, such as DIII-D, the homoclinic tangles resulting from C-coil perturbation of the

separatrix are of particular interest. These separatrix tangles provide *the* mechanism for the nondiffusive escape of hot particles. The locations where their lobes hit the walls of the vacuum vessel (magnetic footprints) are expected to be places where an abundance of hot particles hit. We offer two suggestions for physical verification of this phenomenon: First, comparing heat distributions across the walls of the vacuum vessel with the places where tangle lobes hit the walls, including a search for the spiral structure of heat buildup, as predicted in Ref. 15 and by our calculations. Second, determining whether the bifurcation described above can be observed through a sudden increase in heat on the upper walls of the vessel when the C-coil perturbation amplitude is increased past a certain level, $A(dr_{sep})$.

Since the other studies of magnetic footprints in tokamaks have all involved relatively simple equilibria,^{5,14,15} their predictions may be somewhat less satisfactory when directly compared with experimental data. Our TRIP3D_MAP model is a realistic model of the magnetic field in DIII-D, therefore, with further work, we expect that we will be able to verify our numerical predictions with actual experiments.

ACKNOWLEDGMENTS

The authors would like to thank J. M. Greene for his careful reading of this paper and the referee for his helpful comments.

This is a report of work supported by the U.S. Department of Energy under Contract No. DE-AC03-99ER54463 and by a NDSEG Fellowship, and a National Undergraduate Fusion Fellowship.

¹A. Lichtenberg and M. A. J. Lieberman, *Regular and Chaotic Dynamics*, 2nd ed. (Springer-Verlag, New York, 1992).

²M. V. Berry, in *Topics in Nonlinear Dynamics: A Tribute to Sir Edward Bullard La Jolla Institute* (American Institute of Physics, New York, 1978), pp. 16–120.

³J. D. Meiss, *Rev. Mod. Phys.* **64**, 795 (1992).

⁴R. K. W. Roeder, T. E. Evans, and B. Rapoport, *Bull. Am. Phys. Soc.* **46**, 39 (2001).

⁵E. C. daSilva, I. L. Caldas, R. L. Viana, and M. A. F. Sanjuán, *Phys. Plasmas* **9**, 4917 (2002).

⁶T. E. Evans, R. A. Moyer, and P. Monat, *Phys. Plasmas* **9**, 4957 (2002).

⁷J. L. Luxon, *Nucl. Fusion* **42**, 614 (2002).

⁸L. Lao, H. St. John, R. D. Stambaugh, A. G. Kellman, and W. Pfeiffer, *Nucl. Fusion* **25**, 1611 (1985).

⁹J. D. Hanson, *IEEE Trans. Plasma Sci.* **27**, 1588 (1999).

¹⁰R. Balescu, M. Vlad, and F. Spineanu, *Phys. Rev. E* **58**, 951 (1998).

¹¹S. S. Abdullaev, *Phys. Rev. E* **62**, 3508 (2000).

¹²L. Kuznetsov and G. M. Zaslavsky, *Phys. Rep.* **288**, 457 (1997).

¹³M. J. Schaffer, B. D. Bray, J. A. Boedo *et al.*, *Phys. Plasmas* **8**, 2118 (2001).

¹⁴S. S. Abdullaev, T. Eich, and K. H. Finken, *Phys. Plasmas* **8**, 2739 (2001).

¹⁵N. Pomphrey and A. Reiman, *Phys. Fluids B* **4**, 938 (1992).

¹⁶T. E. Evans, C. J. Lasnier, D. N. Hill, A. W. Leonard, M. E. Fenstermacher, T. W. Petrie, and M. J. Schaffer, *J. Nucl. Mater.* **220–222**, 235 (1995).

¹⁷D. N. Hill, T. Petrie, M. Mahdavi, L. Lao, and W. Howl, *Nucl. Fusion* **28**, 902 (1988).

¹⁸H. J. Poincaré, *Les Méthodes Nouvelle de la Mécanique Céleste* (Gauthier-Villars, Paris, 1892, 1893, 1899), Vols. 1–3, Sec. 397 (reprinted by Librairie Albert Blanchard, Paris, 1987).